T. H. P. Chang M. Hatzakis A. D. Wilson A. J. Speth A. Kern H. Luhn

Scanning Electron Beam Lithography for Fabrication of Magnetic Bubble Circuits

Abstract: A high-resolution technique is described for the experimental fabrication of Permalloy patterns for magnetic bubble circuits having linewidths as small as 3000 Å. The system includes a computer-controlled electron beam, automatic registration, a modified field-stitching method, and exposure control to compensate for proximity effects. Patterns are formed either by electroplating or by evaporation. The system can be used either for directly writing on bubble wafers or for fabricating masks for x-ray or conformable-mask printing.

Introduction

Conventional photolithographic techniques for fabricating magnetic bubble circuits are limited in resolution to minimum linewidths of somewhat above one micrometer, which corresponds to a packing density of 2.8×10^6 bits/in.² or 4.3×10^5 bits/cm² for typical T-I bar devices. The economic advantages of increasing the packing density are important because the cost of processing a single wafer is generally considered to be constant. Scanning electron beam fabrication techniques have been evaluated as an alternative to photolithography because their resolution capabilities have been demonstrated in several areas of fabrication [1-3]. As is shown here, Permalloy patterns can be defined with electron beam lithography with linewidths of 3000 Å and a corresponding packing density of 10^8 bits/in.² or 1.5×10^7 bits/cm² can therefore be achieved.

Electron beam fabrication offers several important advantages for lithography, including a capability of generating geometries smaller than one micrometer, a high adaptability to automation, and the ability to write directly on wafers without the need for a mask.

In addition, the scanning electron beam lithography can be utilized for fabrication of the masks necessary for other high-resolution lithographic technologies that are being developed, such as ultraviolet-light conformable mask printing [4, 5], x-ray printing [6, 7], and electron beam projection printing [8].

Improvements in high-resolution electron beam fabrication methods in two areas are discussed here. The first

is the electron beam system and its computer-controlled functions; the high-speed, high-resolution features; its automatic registration design; the technique of path stitching to very large fields; and exposure control to compensate for proximity effects. The second is electron sensitive resist and the processing techniques that permit formation of metallic patterns either by electroplating through the resist or by evaporation, the "liftoff" method.

Electron beam system

A computer-controlled electron beam system [9] has been developed to explore the potential for achieving high resolution with this new approach to circuit lithography. The design objective was to provide an easily operated system with a capability of generating linewidth patterns in the range of one micrometer and smaller over a field size of at least 2000 fabricated lines up to 4 mm square. The system is intended for the generation of complex present-day microcircuit patterns and should therefore be able to handle a variety of pattern geometries and shapes and at the same time maintain sufficient flexibility to allow various pattern fidelity improvement techniques to be readily incorporated. Last but not least, the system should have the potential for good throughput.

Figure 1 is a block diagram of the system showing the computer, digital and analog electronic controls, and a cross section of the electron optical column. The design

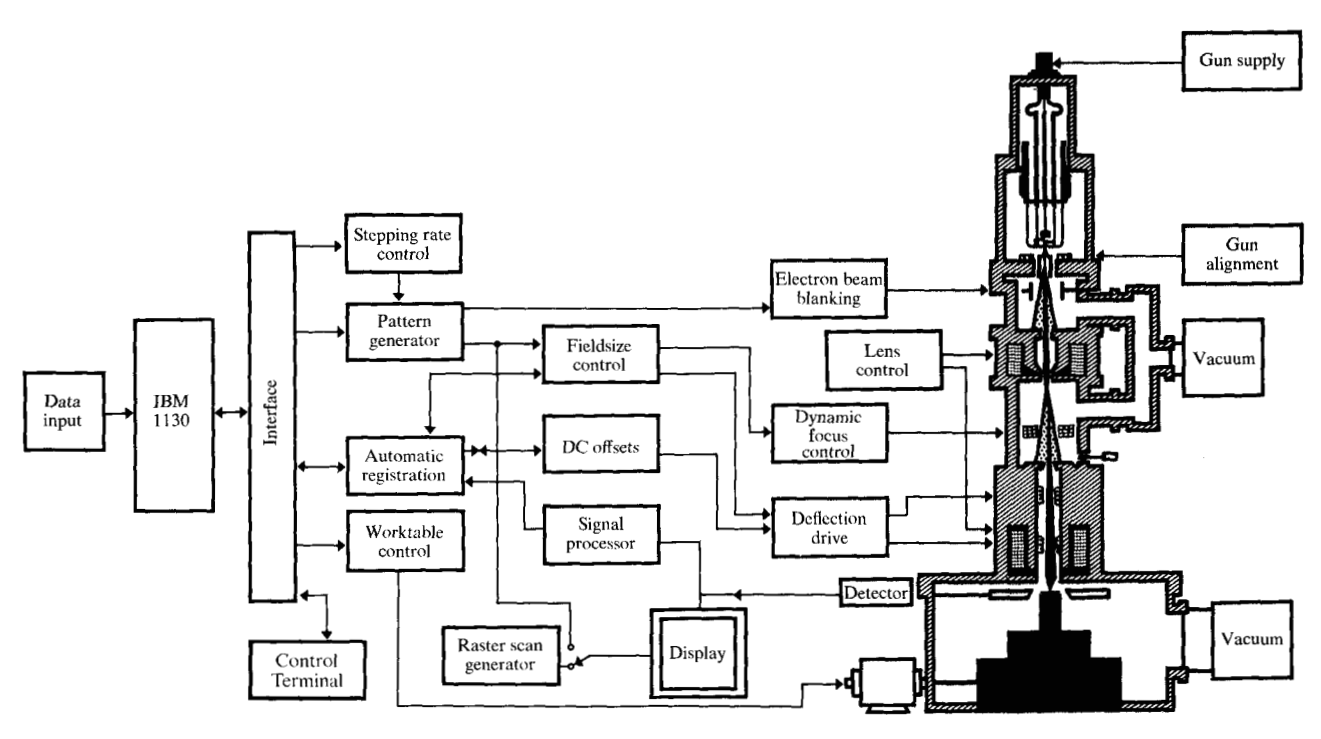


Figure 1 Conceptual diagram of computer-controlled electron beam system. (From Ref. 9).

objectives for the system have been achieved and the system has been used for various experiments, including direct device exposures of 8 K and 16 K bubble memory chips [10, 11] and 8 K FET memory chips [12]. Exposures have also been processed to allow mask fabrication for bubble devices using x-ray and conformable mask printing systems.

• Electron optical column

The column consists of a LaB₆ gun [13] and uses two magnetic lenses to form a finely focused beam of electrons. The beam is scanned by an electromagnetic deflection unit to generate the required patterns. The electron beam diameter can be varied by changing the focal lengths of the magnetic lenses to cover a range of sizes from 0.05 μ m to several micrometers, and it is generally adjusted to approximately one-quarter of the minimum pattern linewidth to ensure good line definition. An electrostatic beam blanking unit is immediately adjacent to the gun to switch the beam on and off at high speed. An electron detection unit is installed in the workchamber to collect signals from the surface of the samples for purposes of beam focusing and registration. A precision x - y table with high-speed stepping motor drivers is also provided to allow the sample surface to be fully

One of the major considerations of the column design is that of the final lens and deflection coil. The final lens in the system is designed for a focal length of five cm. A

double deflection system is used, the entire deflection unit being housed inside the lens bore. Careful computer analyses [14] were performed to study the interaction between the focusing field and the deflection field. It was found that the optimum design would require the lower deflection coil to be placed close to the lens gap, a proper twisting angle between the upper and lower coils, and proper placements of the coil members. As a result the system has a performance which greatly exceeds the initial objective of a field size of 2000 times the minimum pattern linewidth (e.g., 2 mm × 2 mm field for one- μ m lines) for a beam convergent angle of 6×10^{-3} radians and no dynamic focus corrections. In addition, special attention has been given to the problem of eddy current effects associated with a magnetic deflection, because these effects must be fully suppressed for satisfactory operation.

The electron beam forming system has the configurations shown in Fig. 2, and the beam current I(in A) for a beam diameter D(in cm) for the on-axis case can be expressed as

$$I = 3.58\alpha^2 \beta \left[D^2 - (\frac{1}{2}C_s\alpha^3)^2 - \left(C_c \frac{\Delta V}{V}\alpha\right)^2 \right],$$

where α is the beam convergent angle in radians; β is the gun brightness in Acm^{-2} sterad⁻¹; C_s is the spherical aberration coefficient of the final lens in cm.; C_c is the chromatic aberration coefficient of the final lens in cm.; ΔV is the energy spread of the beam in volts; and V is

377

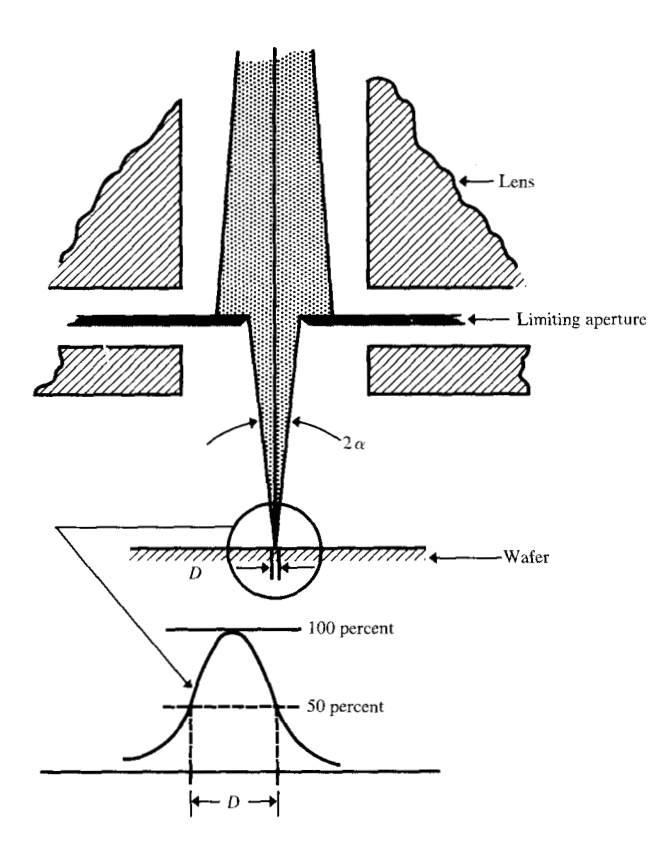


Figure 2 Configuration of the electron beam forming system. An analytic expression for the beam current for the on-axis case is given in the text.

the accelerating energy of the beam in volts. This expression shows that the beam current increases with an increase of gun brightness and with a decrease of lens aberrations. It also indicates the importance of beam convergent angle α , which affects the beam current approximately in the square power. In principle, it is possible to optimize the value of α to produce a maximum value of 1. However, such optimization should be treated with some care, because it is often not possible to use the relatively large α value called for by the optimization without at the same time introducing excessive deflection aberrations and thus limiting the field size. The specific value of α to be used depends on the performance of each individual lens and deflection system and the acceptable tradeoff between beam current and field size for each particular application. In the present system, an α value of 6×10^{-3} radian [14] was chosen as the initial goal.

The exposure time T (in s) to expose a given field size of area A (in cm²) with a resist coating of sensitivity S (in coul/cm²) is given simply as T = AS/I.

The performance of the system can therefore be evaluated using the following typical parameters for the gun, the lens, and the field size: β = 1 × 10⁶ Acm⁻¹ sterad⁻¹ for LaB₆gun C_s = 5 cm C_c = 10 cm

Beam diameter = $\frac{1}{4}$ of minimum pattern linewidth L, and Field size = 2000 L

Typically, for a beam diameter of $\frac{1}{4} \mu m$, the beam current is approximately 8×10^{-8} A, and this is used to expose a one-micrometer linewidth pattern over a 2-mm square field. The exposure time T will depend on the resist sensitivity S, and for $S = 1 \times 10^{-5}$ coul/cm², the value of T is five s for a system using a raster scan to cover every point in the field. However, for the vector scan technique used in the system, the beam is directed only to the pattern areas, and the exposure time can therefore be reduced according to the percentage of pattern area coverage. For an average of 30 percent coverage, the exposure time T (vector), is reduced from 5 s to approximately 2 s. Because the beam current and field area both increase with the square of the beam diameter, the exposure time remains fairly constant for all field sizes, provided the ratio of field size to pattern linewidth is kept constant (i.e., FS = 2000 L).

These results describe the performance of the electron optical column using relatively conservative values of α and S. One can see that considerably higher speed can be attained if some of the more recently achieved values of α and S are used. It should be pointed out that for the exposure time indicated above, the corresponding stepping rate of the beam will be in the 10-MHz region. This will require special attention in the design of digital-to-analog converters and deflection amplifiers.

• Pattern generation

A vector scan technique [15] is used in the system for pattern generation. In this technique, the pattern is first decomposed into a series of basic cells. The system then exposes each field by serially filling in these pattern cells, whose size, geometry and sequence were determined by an offline data processor. Fill-in is performed by line scanning the electron beam within the boundary of each cell. The cell geometries most commonly used are rectangles and parallelograms.

This approach to pattern exposure has several attributes. It is time-efficient because the electron beam is addressed only to the pattern areas to be exposed. It is efficient in the size of data base required to describe the pattern. Also, the fidelity of the exposed pattern can be controlled by using a combination of several exposure adjustment methods, such as the "proximity effect" compensation technique, which is discussed subsequently.

The address resolution of the pattern field is 14 bits for each axis. Each cell is defined by up to five binary

words (the IBM 1130 computer has a word length of 16 bits). Two words are used to define the corner coordinates of the cell, two for the cell dimensions, and the fifth for coding parallelogram shapes and other control functions. Due to the repetitive nature of most of the patterns, substantial data compaction is attained by off-line sorting algorithms used in data preparation. For bubble patterns that generally consist of only a very few basic elements such as T-I bars and chevrons, a very significant data compaction can be readily achieved.

Data are transferred asynchronously from the IBM 1130 to the pattern generator, which is a hardware unit designed to generate a sequence of line scans to fill in rectangles and parallelograms. The rate at which the individual pattern cells are exposed is controlled by the scan rate clock. Counting circuitry in the pattern generator drives two 14-bit D/A (digital-to-analog) converters, one for each deflection axis. The D/A outputs, after attenuation by the field size control unit, drive the deflection amplifier. Fine field adjustments (size, offset, rotation, and orthogonality) have been instrumented and are used for setup and registration. The address resolution of the D/A converters can be changed by the computer from its normal 14-bit resolution to 13-bit and lower resolutions. This means that patterns can be exposed either in 14- or 13-bit resolution. The advantage of this capability in relation to registration will be discussed in a subsequent section.

Rectangles and parallelograms can both be filled using bidirectional raster scan. In the case of rectangles, another fill-in sequence is possible and is most often used. This is illustrated in Fig. 3 and is called the framing (or spiral) scan. In both techniques, the scan rate for each individual cell can be readily adjusted to provide a compensation for the proximity effect introduced by adjacent pattern cells. The framing (or spiral) scan provides an additional adjustment for scan rate within the cell or the ability to introduce additional scan lines near the edges (not shown in Fig. 3) to compensate for the proximity effect on the edges.

· Automatic registration and field stitching

A computer-controlled automatic registration system [16] has been developed to enable accurate exposure of overlay patterns. The system uses digital signal enhancement techniques to improve the signal/noise ratio of the registration mark signals. Registration overlays have been made with absolute errors on the order of 100 ppm, i.e., a level-to-level error of about \pm 0.1 μ m for a 2-mm field. The system is illustrated in Fig. 4.

To detect registration marks covered with resist, it has been found [17] that the backscattered electrons provide a better and more reliable signal than the secondary electrons. For this reason a detector suited for the detec-

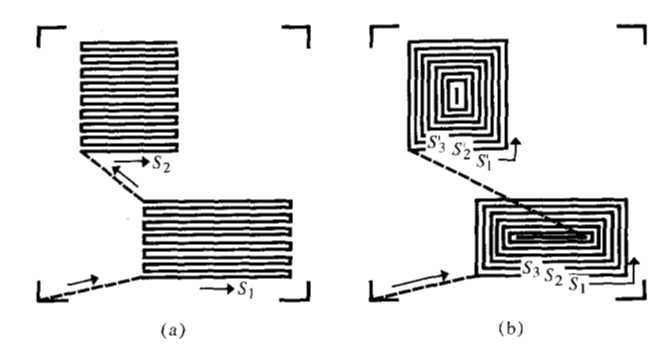


Figure 3 Two methods of vector scan for pattern generation.

(a) The bidirectional raster fill-in scan. (b) The spiral fill-in scan, which can be adjusted for scan rate within the cell and can add scan lines to compensate for proximity effect. S indicates scanning speed.

tion of high energy electrons, such as a grounded scintillator detector, is normally used. The detector system is housed in a flat pancake-like structure located between the final lens and the wafer, and the signals from a pair of scintillator detectors are transmitted through light pipes to photomultipliers (PMT) located outside the vacuum chamber. An independent pair of secondary electron detectors is also provided to compare the two types of signals.

When an electron beam scans a registration mark, the signal will take the form shown in Fig. 4(b). It can be seen that the noise in the signal can introduce an error in the position of the edge of the mark. Furthermore, it can also be seen from the same figure that the amount of this noise-induced error is dependent upon the rise slope of the signal. In general a faster rise slope can tolerate a higher noise level. If the noise distribution is taken as Gaussian, one can show that the probability of the noise to have an instantaneous value of $v > \chi$ is given by

$$P(v > \chi) = \frac{1}{2} \left(1 - \operatorname{erf} \frac{\chi}{\sigma \sqrt{2}}\right),$$

where $P(v > \chi)$ is the probability that the instantaneous noise value will be equal to or greater than χ , and σ is the rms value of the noise. It has been shown [16] that for a probability value P of 1/100000 (a probability equivalent to about four sigma), the corresponding value of χ/σ is 4.25.

Figure 4(c) shows four cases of signal with the rise slope of the signal equal to 2, 3, 4, and 8 beam incrementing steps. The actual rise slope of a signal that can be achieved in practice will depend partly on the edge slope of the registration mark and partly on the effective beam diameter, which can be considerably larger than the incident beam because of the scattering effect in the resist layer. The best accuracy one can aim for is that the noise error be equivalent to one beam incrementing step,

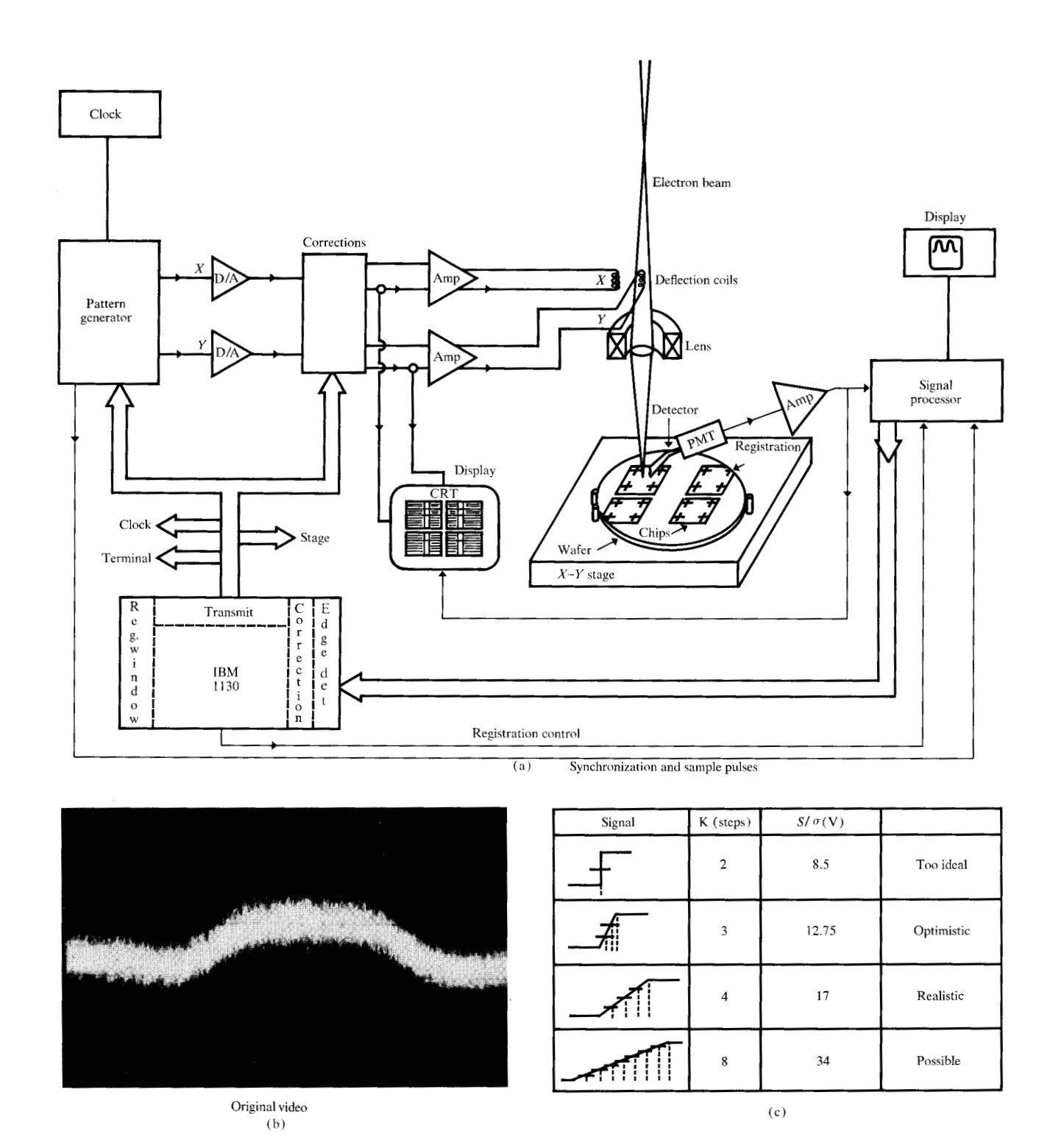


Figure 4 The automatic registration system. (a) Conceptual diagram. (b) Form of video signal as electron beam scans a registration mark. (c) Four cases of the scan signal when the rise slope depends on two, three, four, and eight beam incrementing steps.

and if the probability for this is set at 1/100000, the required signal/noise ratio for the four cases can be derived as shown in Fig. 4(c). In practice, it is found that a risetime equal to four beam steps is probably more

realistic, and this indicates a required signal/noise ratio of 17. This result demonstrates the need of some form of signal/noise enhancement, as the actual signal/noise ratio observed in practice can be as low as 3.5.

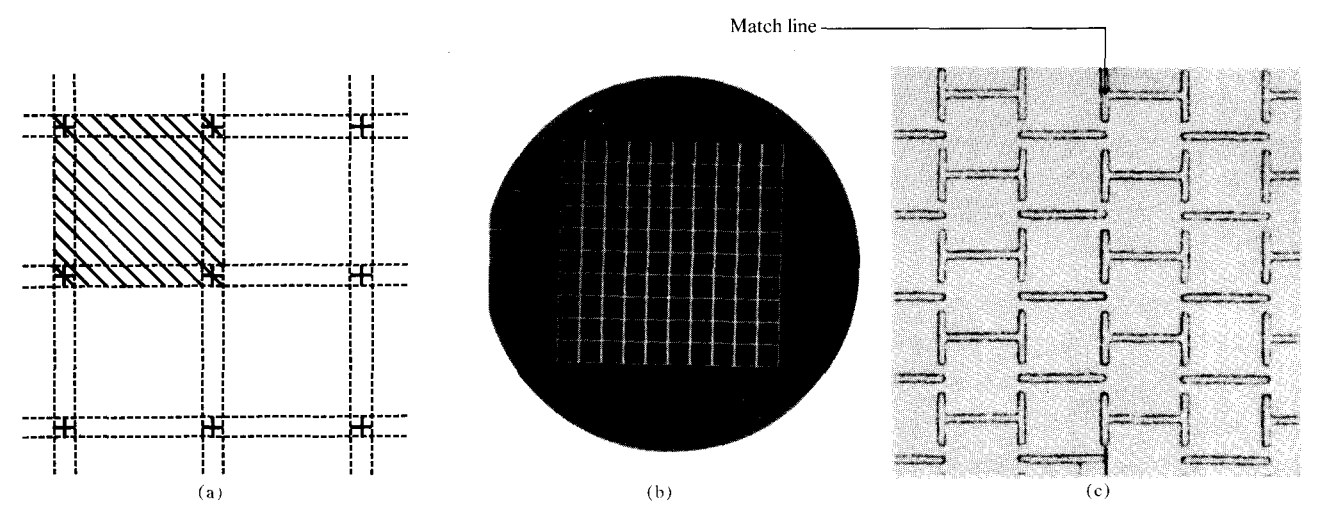


Figure 5 Field-stitching technique. (a) Basic principle. (b) A chip 1.89×1.89 cm, generated by stitching a 10×10 array of 1.89 mm square subfields, with one- μ m T-1 bars at one- μ m gaps. (c) Enlarged view of the boundary.

To achieve the 100 ppm accuracy mentioned earlier, it is necessary to refine the beam incrementing step. This is done by halving the beam step distance during registration. In practice the computer simply switches the D/A output from 13 bits/field (approx. 8000 beam steps per axis) for pattern generation, to 14 bits/field (approx. 16000 beam steps per axis) for registration.

A schematic of the registration system is shown in Fig. 4(a). The signal processor uses digital signal enhancement techniques to improve the video signal/noise ratio. Signals of a series of scans across the same mark are sent to the signal processor which digitizes the signals and performs summing and averaging functions. As a result of this the signal/noise ratio is improved by a factor equal to the square root of the number of scans used. The improved data is read into the computer, which performs the computation for all the corrections (size, offsets, rotation, and orthogonality) and applies these corrections to the deflection system by way of the analog control units.

One important application of this automatic registration system for bubble technology is in the enlargement of chip size by the use of a modified field-stitching technique. Figure 5(a) showns the basic principle of this method. It shows that the enlargement of chip size is achieved by accurately butting adjacent fields using registration marks. Successful demonstration of this technique is presented in Fig. 5(b), which shows 1.89×1.89 cm chip obtained by stitching a 10×10 array of 1.89-mm square subfields containing one- μ m linewidth T-I bars. Figure 5(c) is a magnified view at the boundary of two of the abutting fields, and it can be seen that no measureable stitching error can be detected. This result demonstrates not only the accuracy of the registration

system but also the linearity of the deflection system, i.e., the absence of either pin-cushion or barrel distortion at the 2-mm square field. The potential of this field-stitching technique for large bubble memory chip can be important. For example, the 1.89-cm square field described here could have a memory capacity of approximately 5×10^6 bits for two- μ m bubbles, and larger field size can be readily achieved using more registration marks and a larger wafer size.

This brief description of the electron beam system is now followed by a discussion of the electron resist processes.

Electron resist processes

The fabrication of magnetic bubble circuits depends largely on the delineation of a Permalloy (NiFe,) pattern used for bubble propagation. This pattern consists of arrays of T-I or Y-I bars, or other configurations with line widths equal to the bubble radius and spacing approximately half of the bubble radius. Typically, the Permallov thickness should be at least 2500 Å, even if the bubble radius is of the same order of magnitude. For instance, propagation of one-micrometer bubbles requires Permalloy patterns with 0.5 μ m linewidth, 0.25um spacing and at least 2500-Å thickness. It is obvious that such a pattern cannot be defined easily through subtractive etching of blanket Permalloy film because of undercutting effects, especially if chemical etching is used. The alternative is some form of additive metallization through a resist mask exposed and developed by electron beam. This can be accomplished by metal evaporation technique or by electrolytic plating of the metal. Both of these techniques require the use of a positive resist such as poly-(methyl methacrylate), known

381

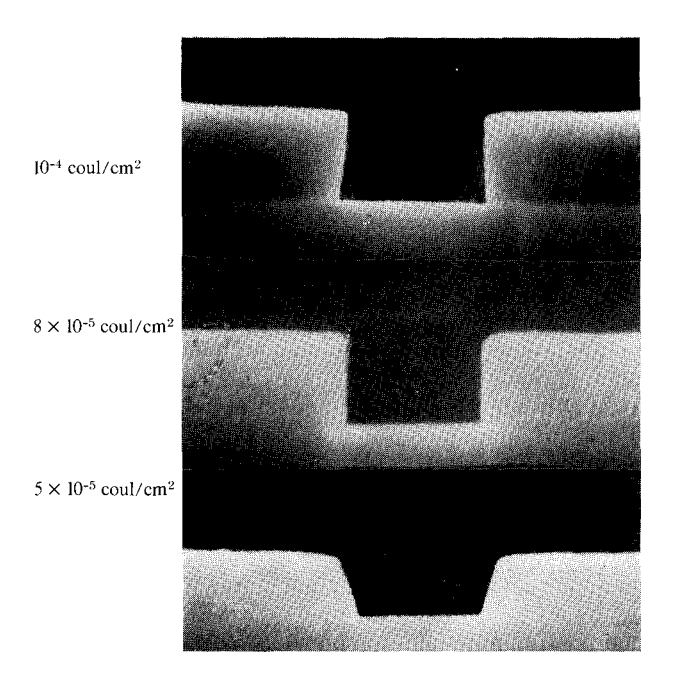


Figure 6 Change of developed resist line from undercut to overcut as more resist is dissolved from top edges. PMMA resist profiles, exposed at 25 kV, for exposures in charge per unit area expressed in units of coul/cm²: (a) 10^{-4} , (b) 8×10^{-5} , and (c) 5×10^{-5} . Development was in methyl isobutyl ketone.

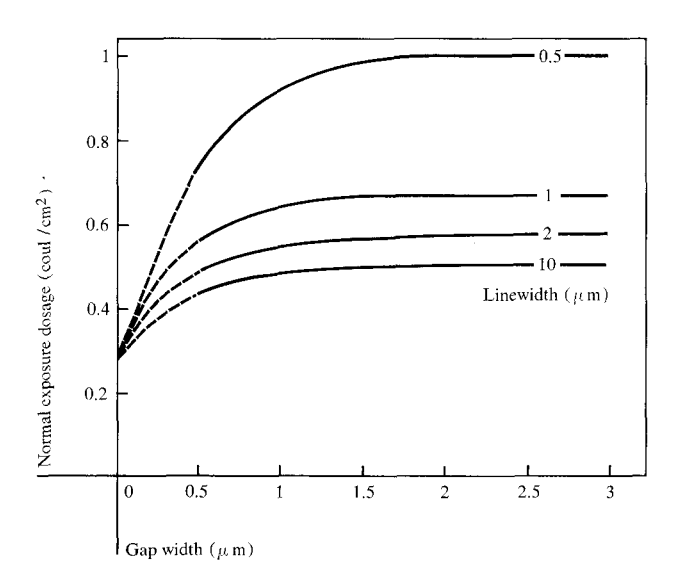


Figure 7 Requirement of optimum exposure dosage for given linewidths and gap spacings. (See Ref. 24).

as PMMA [18, 19]. Electron resists, like photoresists, are divided into two major categories; the negative resists that crosslink and remain in the area exposed to the beam after development, and the positive resist that degrade and are removed in the area exposed by the beam. The electron beam exposure characteristics of these resists

have been described elsewhere [13], and it was shown that, in general, negative resists are not suitable for high resolution work, especially with any additive metallization scheme. Negative resists however, are generally faster than positive resists, and their use has been suggested in combination with ion milling in cases where throughput is more important than resolution. Any process developed for magnetic bubble fabrication should be extendible to the very small linewidths and high packing densities. For this reason, positive resists such as PMMA are preferred and have been carefully evaluated. This resist, together with an additive metallization process, has demonstrated a resolution capability of better than 1000-Å linewidths [20]. Additive metallization through an exposed and developed resist mask can be accomplished either by evaporation or sputter deposition of the metal (known as the "liftoff" technique) or by electroplating the metal onto a conductive layer previously deposited under the resist. Success or failure of any additive metallization method depends on several factors such as surface preparation, resist thickness, and developed resist profile. These are discussed here as they apply to the method of metallization used.

• Liftoff by evaporation or sputter deposition

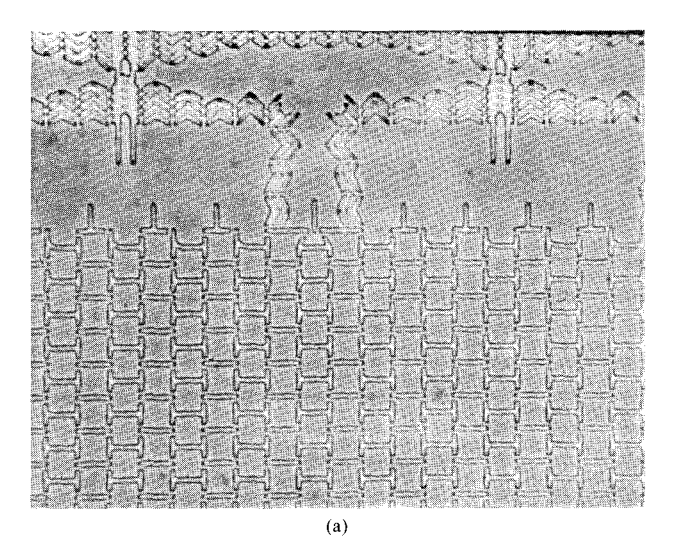
One of the most important characteristics of positive electron resists is that electron beam exposure above a certain charge density produces some undercut in the resist edge after development. The amount of undercut (negative edge slope) depends on the exposure charge density, resist thickness, and beam accelerating potential. This undercut is caused primarily by electron scattering in the resist and substrate. These scattering effects have been studied experimentally and theoretically [21, 22]. Although an undercut profile is desirable, because it is essential for the liftoff process, excessive undercut should be avoided. This is true because too much undercut, especially in resist layers thicker than 6000 Å, can impose a limit to the minimum distance between lines if a merging of lines at the bottom of the resist layer is to be prevented. The scattering effect and therefore the undercut profile is more pronounced at lower beam accelerating potentials. A good way to compare the relative merits at various beam accelerating potentials is to measure the maximum depth-to-width ratio that can be obtained in the exposed and developed line at different potentials. It has been shown experimentally that a higher depth-to-width ratio is generally obtained at the higher beam accelerating potentials of the order of 25 kV, while sufficient undercut is maintained for liftoff metallization.

Another important factor in determining undercut is the exposure dosage of the resist. Exposure is customarily measured in charge per unit area (coul/cm²) which is sufficient if the resist thickness is also specified. For high exposure charge densities, the electron beam scattering effect dominates the developed profile. However, at lower exposure charge densities, the effect of the developer becomes increasingly important because the differential resist solubility between exposed and unexposed regions decreases with decreasing exposure. As a result, the shape of the edge of developed resist lines changes drastically from undercut to overcut as more resist is dissolved from the top edges of the exposed region. This is illustrated in Fig. 6, where developed PMMA resist profiles exposed at 25 kV at 10^{-4} , 8 \times 10^{-5} and 5×10^{-5} coul/cm² are shown. The change from undercut to overcut can be easily seen as well as the exposure at which vertical resist walls are obtained. It is clear from the illustrations that to obtain undercut sufficient for liftoff, a charge density of 10^{-4} coul/cm² or more must be used at 25 kV.

The minimum resist thickness necessary for liftoff depends on the metal thickness to be evaporated or sputtered; in general, the resist thickness must exceed the metal thickness in order to maintain a discontinuity between the metal deposited on the substrate through the resist and the metal deposited on top of the resist. Clearly if this discontinuity is not maintained, liftoff will be impossible. As a rough guide for an undercut angle of −5° with the surface normal, this thickness margin should be at least 30 percent of the metal thickness. One of the most serious problems of the liftoff process is poor metal adhension to the substrate. Metallization techniques requiring high substrate temperature cannot be used because the substrate temperature has to be maintained below the glass transition temperature of the resist, or the temperature at which the resist will flow and distort the developed image. For PMMA, the resist temperature during any stage of the metal deposition should be kept below 100°C, and at this temperature the adhesion of many metals is poor unless special surface cleaning techniques are used after resist development. If the metal is deposited on a silicon dioxide layer, as is the case in bubble propagation circuits, then the easiest way to obtain a clean surface is to etch a thin layer of SiO₂ in the areas where the resist is removed after development. This is done by dipping in a dilute buffered HF solution and rinsing with deionized water prior to the metal deposition. The etch method is particularly important in cases of high pattern density of narrow line widths and thick resist layers when it is difficult to rinse resist residue from the exposed SiO_o surface by spraying with alcohol or water.

To summarize then, successful liftoff requires:

1. Exposure between 20-30 kV for high aspect ratio patterns.



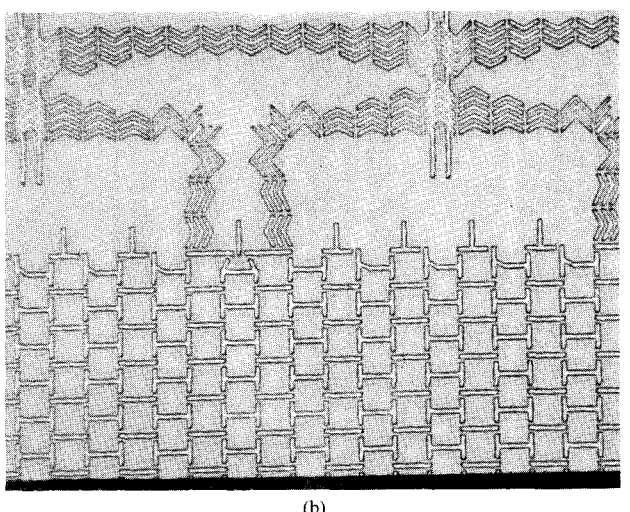


Figure 8 Example of "proximity effect," where various areas on a bubble pattern require separate resist exposures. (a) Uncorrected pattern. (b) Pattern generated with automatic adjustment of exposure to compensate for proximity effects.

- 2. Exposure charge density higher than 10^{-4} coul/cm² at 20-25 kV.
- 3. Maintenance of resist thickness at 30-50 percent higher than the metal thickness.
- 4. Maintence of substrate and resist surface temperature below 100°C during metal deposition.
- 5. Use of some form of surface cleaning prior to metallization, preferably a chemical process that does not affect the resist.
- Electroplating of metals through the resist pattern
 The main advantages of electroplating over liftoff is that
 the metallic pattern can be deposited to a thickness
 equal or in some special cases, even greater than the resist thickness. No undercut is required and the metal
 thickness-to-width ratio can be higher than that obtainable with liftoff. In addition, metal adhesion is better if

the substrate surface is clean. Unfortunately, good cleanliness is not achieved as easily as with liftoff because a thin metal layer must be maintained under the resist for subsequent electroplating. This cannot be chemically etched prior to plating because the metal layer is usually very thin. In magnetic bubble circuits, this layer is usually 200-300 Å of Permalloy, evaporated on the SiO_2 spacer. During electroplating, electrical contact is made to this Permalloy layer and additional Permalloy or gold is deposited in the areas where the resist has been removed during development [23].

Resist undercut is not only unnecessary in plating but can be detrimental to the process because the developed resist lines are wider at the bottom than at the top. Consequently, as the metal is deposited on the substrate, the metallic linewidth is forced to decrease in order to conform to the resist profile. This generates an upward force on the edges of the resist and can, in some cases, lift the narrower resist lines from the substrate, thus destroying the pattern. Therefore, in order to avoid undercut in any part of the pattern exposed on the resist, the exposure charge density must be accurately controlled to a level of 10^{-4} coul/cm² or below at 20-25 kV for PMMA resist, as shown in Fig. 6.

Another advantage of electroplating is that it is a low temperature process and therefore thermal stability is not required for the resist. An exposed substrate surface can be cleaned after resist development by some method of ion etching that removes a uniformly thin layer of resis from all parts of the pattern, including any possible resist residue from the exposed substrate. To accommodate this resist removal, the initial resist thickness has to be slightly higher than that of the metal after plating. One of the main disadvantages of plating is that the uniformity of metal thickness over the entire wafer and the alloy composition are difficult to maintain. Also it is not possible to electroplate many metals and alloys that can be easily deposited by evaporation or rf sputter deposition.

In general then, for plating it is required that

- 1. The exposure charge density should be accurately controlled so that no excessive resist undercut exists anywhere in the developed pattern. ($< 10^{-4} \text{ coul}/\text{cm}^2$).
- 2. Resist thickness can be equal to the metal thickness, although a 10 percent increase in thickness is often provided for the residue cleaning operation.
- 3. Because chemical etching cannot be used, low-temperature ion etching should be used to remove any resist residue in the developed regions.
- 4. A large open area containing no resist must be provided at the edge of the wafer in order to make electrical contact to the thin Permalloy layer during plating.

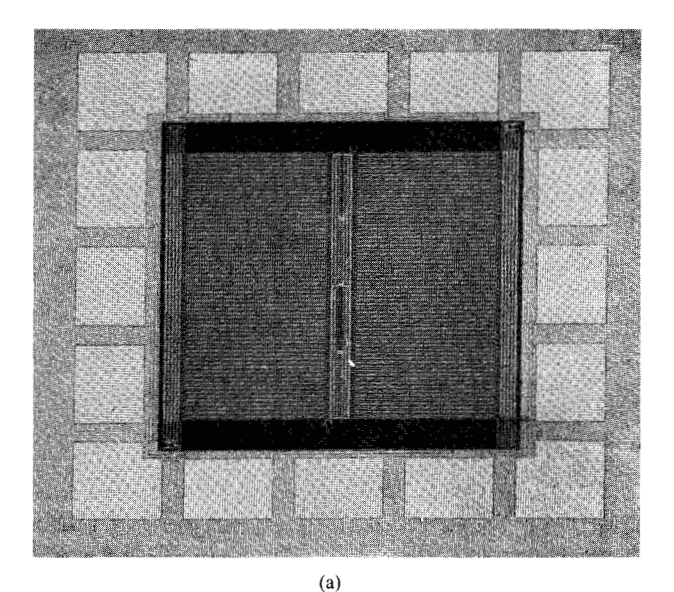
• Proximity effects on resist exposure

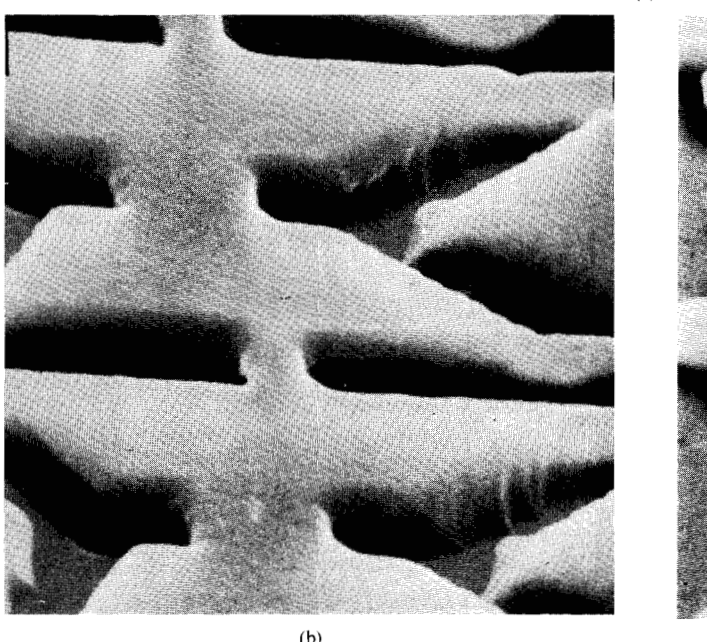
One of the problems observed during any attempt to write complex, high density patterns is that the optimum exposure dosage requirement at different areas of the pattern can differ [24]. This variation depends partly on pattern geometry, e.g., the linewidth, and partly on an effect related to the pattern packing density. Figure 7 shows the variation of exposure dosage as a function of linewidth and packing density (or gap spacing) for a 6000 Å resist (PMMA) on silicon wafer. This variation is mainly due to the contribution of back scattered electrons to the exposure of the resist and therefore it depends on beam accelerating voltage, resist thickness, and substrate material. In general, larger pattern geometries require less exposure dosage than smaller ones, and closely packed patterns also require less exposure than do isolated patterns. In the case of a relatively simple pattern with relatively large geometry, say, above one micrometer, this variation of exposure requirement can usually be accommodated by the exposure tolerance of the resist. However, in the case of complex, high density patterns, especially ones with submicrometer geometries, correct exposure is often not achieved by relying on the resist tolerance alone, and some means of providing automatic adjustment to the exposure is required. It has been found [9] that one effective way of solving this problem is to selectively vary the scanning speed of the beam according to exposure requirements. For the vector-scan pattern generation, where the pattern is divided into a series of small basic elements, the variation of scanning speed for each of these elements can be readily controlled according to need by means of the computer, and the necessary instructions for this variation can be incorporated into the initial pattern data preparation program. Experimental results show that this approach works and has considerably more flexibility than several other possible solutions, such as varying the beam current or tailoring pattern size. The bubble pattern shown in Fig. 8(a) is typical of this proximity problem. It can be seen that the packing density of the pattern in the T-I bar region is substantially less than that in the chevron and transfer gate regions, thus resulting in different exposure requirements for these two areas. The pattern shown in Fig. 8(b) was generated with exposure dosage adjusted automatically by the computer to compensate for proximity effects.

Experimental methods and results

• Sample preparation

Electron beam fabrication of magnetic bubble circuits was carried out on either one-inch diameter $Gd_3Ga_5O_{12}$ wafers with garnet films grown on, or on one-inch diameter glass wafers with evaporated amorphous magnetic





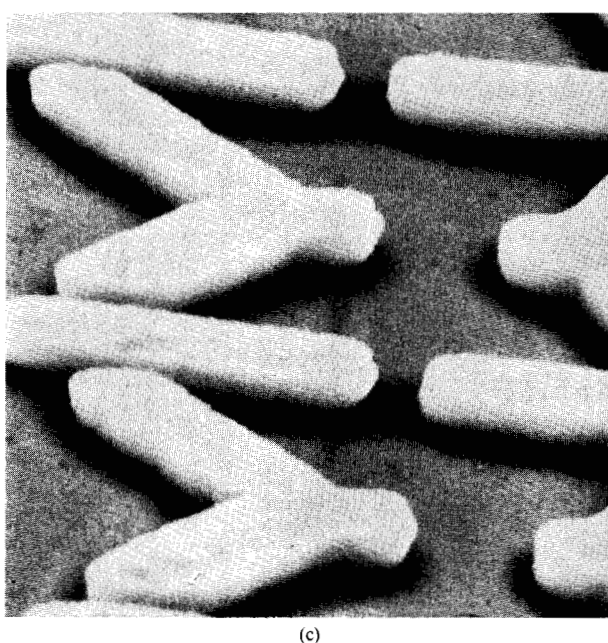


Figure 9 A 16 K bit magnetic bubble memory chip (a) Micrograph of the circuit. (b) Resist pattern of Y-1 bars, one- μ m linewidth. (c) Plated gold on Permalloy pattern, one- μ m linewidth.

films. Both types of wafers had SiO_2 spacers evaporated on and were treated identically as far as the electron beam fabrication process is concerned. Samples intended for electroplating had an additional evaporation of 200-300 Å of Permalloy, which served as the conductor in the plating bath. A commercial PMMA resist was used. The resist was dissolved in chlorobenzene in various concentrations, ranging from 10 to 15 percent to obtain various resist thicknesses in one spinning operation. The wafers were baked at 160°C after spinning of the resist in order to relieve strain in the resist de-

veloped during spinning and also to drive off remaining solvent in the dried film. Resist thickness was measured after baking, using a Watson-type interferometer with polychromatic illumination, over a scratch on the resist film. Wafers intended for plating had a ring of resist removed around the edge of the sample so that contact could be made to the Permalloy undercoat for the plating bath. This resist-free region of the wafer was also used to ground the sample and prevent electrical charging during the exposure. Samples intended for evaporation had to be grounded by removing both the resist and

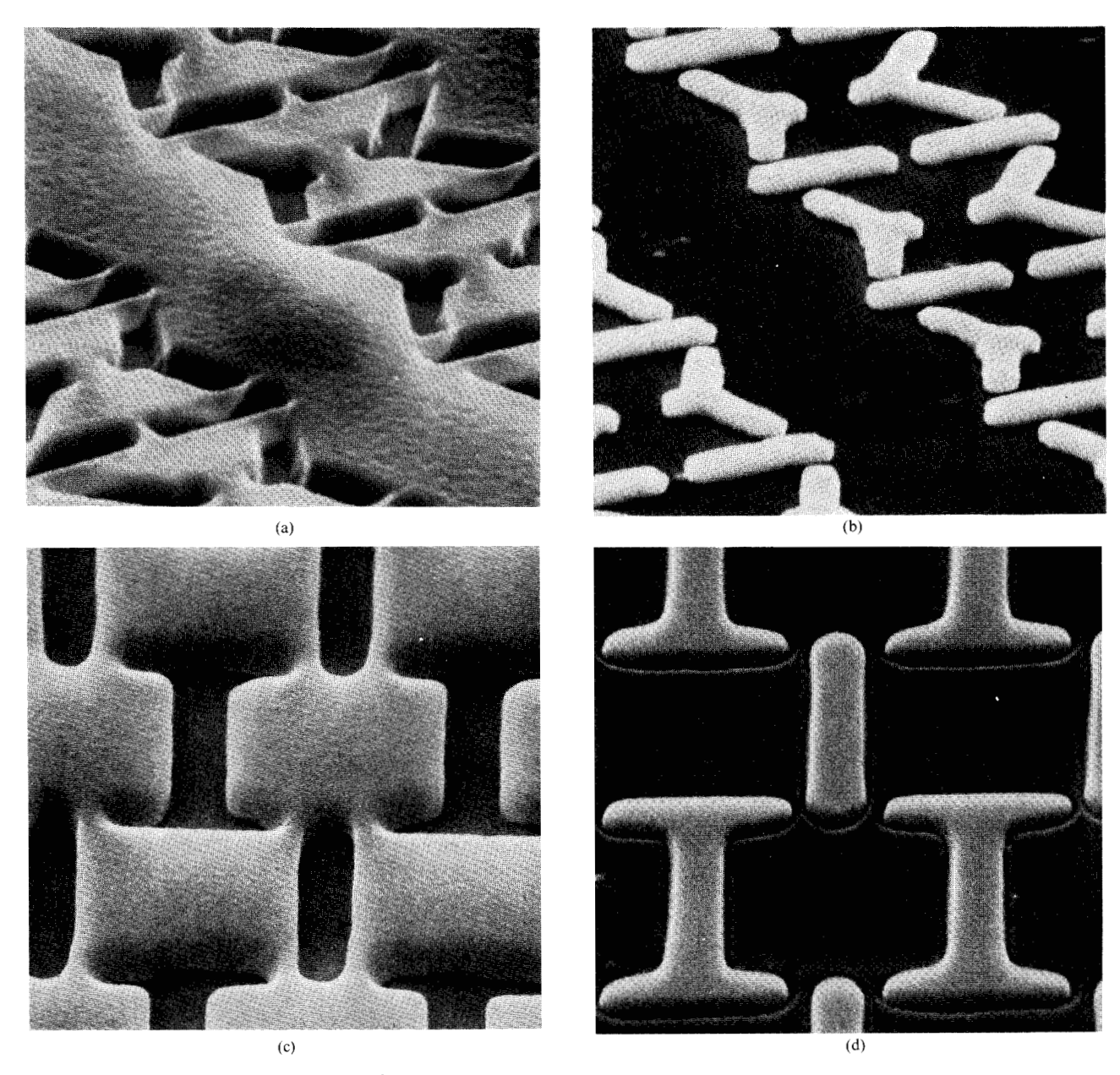
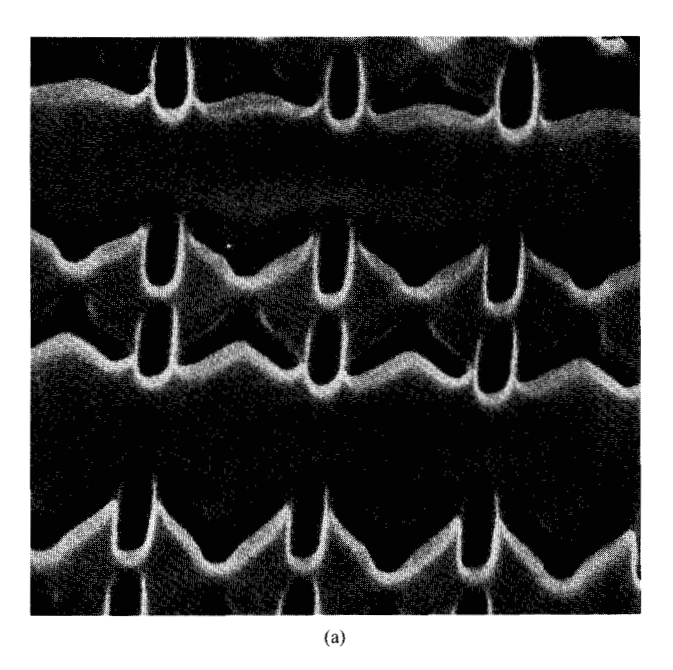


Figure 10 Pattern configuration for 5000 Å linewidth. (a) Resist pattern. (b) Electroplated pattern corresponding to (a). (c) Resist pattern. (d) Metallized pattern corresponding to (c) after liftoff.

underlying ${\rm SiO}_2$ to expose the amorphous conductive magnetic film onto which contact was made with the holder. The nominal exposure charge density was adjusted at $2\times 10^{-4}~{\rm Coul/cm^2}$ for the liftoff samples and $10^{-4}~{\rm coul/cm^2}$ for the electroplating samples. This exposure was further reduced according to the packing density of each section of the pattern by increasing the writing speed as shown in the section on proximity effects.

Development was carried out in a solution consisting of one part methyl isobutyl ketone (MIBK) to one part of isopropyl alcohol, for a time depending on the minimum pattern linewidth, in general, from 30 seconds to two minutes. After development, the pattern quality was studied in an optical microscope at high magnification to determine whether additional development was required. In some cases, especially for the submicrometer patterns, a scanning electron microscope (SEM) was necessary to determine whether the resist pattern was adequately developed.

Samples intended for liftoff were subsequently etched in HF solution to make sure that a clean ${\rm SiO_2}$ surface was obtained prior to metal evaporation.



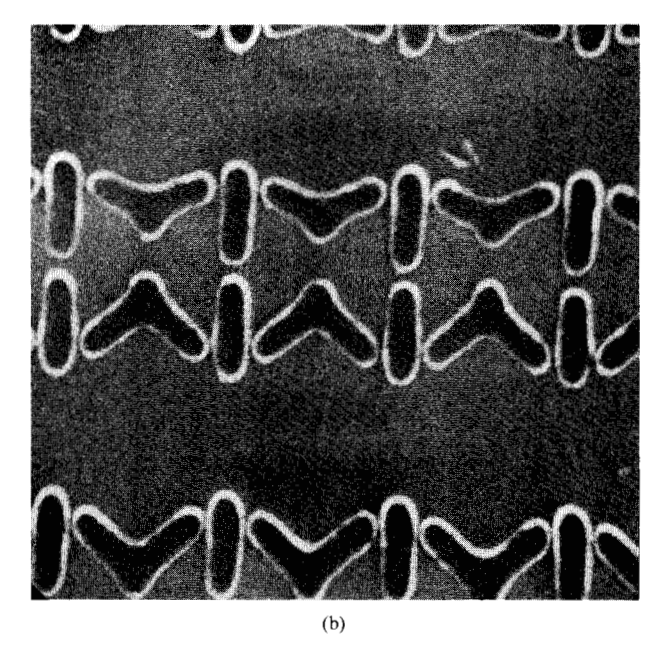


Figure 11 Pattern configuration for 3000 Å linewidth. (a) Resist pattern, 1000 Å minimum spacing. (b) Corresponding metallized pattern after liftoff.

Samples intended for electroplating were cleaned by plasma etching. Evaporation or plating of Permalloy and gold was carried out as described elsewhere [11, 23]. Resist removal or liftoff was accomplished by soaking in hot trichloroethylene for five to ten minutes followed by ultrasonic agitation in trichloroethylene if necessary.

• Results

Several basic bubble propagation patterns were exposed at linewidths of one micrometer or smaller. A micrograph of a 16 K-bit bubble circuit is shown in Fig. 9(a). Figure 9(b) shows the resist pattern of one-micrometer linewidth and Fig. 9(c) the plated Permalloy plus gold with a total metal thickness of 6000 Å. Also Fig. 10(a) shows a 0.5 μ m resist pattern and 10(b) the corresponding electroplated pattern. Similar photographs of resist and metallized patterns after liftoff are shown in Figs. 10(c) and 10(d) for the 0.5- μ m linewidth.

Experimental patterns intended to show extendability of the process to smaller dimensions are shown in Fig. 11(a), an SEM photograph of the resist pattern after development, with resist thickness of 5000 Å, linewidth of 3000 Å, and minimum spacing between Y and I's of 1000 Å. Figure 11(b) shows the corresponding metal pattern after liftoff.

In addition to these experiments, the electron beam process was used to fabricate masks used for x-ray printing and comformable mask printing with deep UV

light. X-ray masks were processed in the same way as samples intended for electroplating on thin substrates stretched over one-inch diameter rings.

Conformable masks for contact printing were made by first evaporating a 1000 Å layer of aluminum on an optically flat quartz or sapphire disc and then applying resist, baking, and exposing in the electron beam system. After development, the pattern was etched in the aluminum layer, in the areas not protected by the resist, by immersion in a phosphoric-nitric acid solution.

Concluding remarks

An electron beam fabrication system has been described, along with the process for producing high-resolution magnetic bubble circuits of micrometer linewidths and smaller. The basic features and performance of a computer-controlled electron beam system were shown in the first part of the paper. This is followed by a description of the procedure for preparing samples. The application of the systems both for the direct writing on bubble wafers and for the making of masks by x-ray and conformable-mask methods was discussed. A number of experimental bubble devices have been fabricated and these include some 16 K-bit circuits with linewidths in the range of one micrometer and smaller.

Acknowledgments

The authors thank W. W. Blair, W. L. Keller, B. Canavello, and T. Donohue for their contributions

387

in the development of the electron beam system and resist processing. The work on the bubble devices was carried out in conjunction with the magnetic bubble group at the IBM Thomas J. Watson Research Center.

References

- M. Hatzakis and A. N. Broers, Record of 11th Symposium on Electron, Ion and Laser Beam Technology, L. Morton, ed., San Francisco Press, San Francisco, 1971, p. 337.
- E. D. Wolf, F. S. Ozeenier, and R. D. Weglein, Proceedings of the 1973 Ultrasonics Symposium, Monterey, CA., J. deKlerk, ed., IEEE, New York, p. 510.
- G. L. Varnell, D. F. Spicer, and A. C. Rodger, J. Vac. Sci. Technol. 10, 1048 (1973).
- H. I. Smith, F. J. Bachner, and N. Efremow, J. Electrochem. Soc. 118, 821 (1971).
- 5. B. J. Lin, IBM J. Res. Develop. 118, 213 (1976).
- H. I. Smith, D. L. Spears, and S. E. Bernacki, J. Vac. Sci. Technol. 10, 913 (1973).
- E. Spiller, R. Feder, and J. Topalian, J. Vac. Sci. Technol. 12, 1332 (1975).
- 8. T. W. O'Keefe, J. Vine, and R. M. Handy, Solid State Electronics 12, 841 (1969).
- T. H. P. Chang, A. D. Wilson, A. J. Speth, and A. Kern, Electron and Ion Beam Science and Technology: Sixth In- ternational Conference, San Francisco. R. Bakish, ed., The Electrochemical Society, Princeton, NJ, 1974, p. 580.
- M. Kryder, K. Y. Ahn, and J. V. Powers, *IEEE Trans. Magn.* MAG-11, 1145 (1975).
- K. Ahn, T. H. P. Chang, M. Hatzakis, M. H. Kryder, and H. Luhn, *IEEE Trans. Magn.* MAG-11, 1142 (1975).
- H. N. Yu, R. H. Dennard, T. H. P. Chang, C. M. Osburn,
 V. DiLonardo, H. E. Luhn, J. Vac. Sci. Technol. 12, 1297 (1975).

- 13. A. N. Broers, J. Sci. Instr. 40, 1040 (1969).
- 14. E. Munro, J. Vac. Sci. Technol. 12, 1146 (1975).
- A. J. Speth, A. D. Wilson, A. Kern, and T. H. P. Chang, J. Vac. Sci. Technol. 12, 1235 (1975).
- A. D. Wilson, T. H. P. Chang, and A. Kern, J. Vac. Sci. Technol. 12, 1240 (1975).
- T. H. P. Chang, *Electron Microscopy 1974*, Abstracts of papers presented to the Eighth International Congress on Electron Microscopy, Canberra, Australia, J. V. Sanders and D. J. Goodchild, eds., 1974, vol. 1, p. 650.
- 18. M. Hatazkis, J. Electrochem. Soc. 116, 1033 (1969).
- I. Haller, M. Hatzakis, and R. Srinivasan, *IBM J. Res. Develop.* 12, 251 (1968).
- M. Hatzakis, Applied Polymer Symposium No. 23, 73 (1974).
- R. J. Hawryluk, A. Soars, H. I. Smith and A. M. Hawryluk, Electron and Ion Beam Science and Technology: Sixth International Conference, San Francisco. R. Bakish, ed., The Electrochemical Society, Princeton, NJ, 1974, p. 87.
- D. F. Kyser and K. Murata, Electron and Ion Beam Science and Technology: Sixth International Conference, San Francisco. R. Bakish, ed., The Electrochemical Society, Princeton, NJ, 1974, p. 205.
- L. T. Romankiw, S. Krongelb, E. E. Castellani, A. T. Pfeiffer, B. J. Stoeber, and J. D. Olsen, *IEEE Trans. Magn.* MAG-10, 828 (1974).
- 24. T. H. P. Chang. J. Vac. Sci. Technol. 12, 1271 (1975).

Received May 29, 1975

The authors are located at the IBM Thomas J. Watson Research Center, Yorktown Heights, New York 10598.